AN INVESTIGATION ON ANISOTROPY OF COSMIC RAYS WITH A SMALL AIR SHOWER ARRAY

M. BAHMANABADI[1*], M. KHAKIAN GHOMI[1], J. SAMIMI[1] and D. PURMOHAMMAD[2]

[1] *Physics Department, Sharif University of Technology, P.O. Box 11365-9161, Tehran, Iran*

[2] *Faculty of science, Imam Khomeini International University, P.O. Box 34194-288, Gazvin, Iran*

(author for correspondence, e-mail: bahmanabadi@sina.sharif.ac.ir)*

(Received 8 April 2003; accepted 9 December 2003)

Abstract. We have studied anisotropy of cosmic rays with an Extensive Air Shower (EAS) array in Tehran 1200 m above sea level. In analyzing the data set, we have used appropriate techniques of analysis and considered environmental effects. An asymmetry has been observed in the azimuthal distribution of EAS of cosmic rays because of magnetic field of the Earth.

Key words: cosmic ray, Extensive Air Shower, anisotropy, geomagnetic field

1. Introduction

The majority of charged cosmic rays ($E \leq 10^{16} eV$) are repeatedly deflected in the $\approx 3\mu$G magnetic field of the Galaxy causing a diffusive transport. This means that positional astronomy is not possible except perhaps at the highest energies. An observer within the Galaxy is expected to observe essentially an isotropic distribution of arrival directions. Deviation from isotropy in the arrival directions of cosmic rays on Earth are expected due to the earth movement relative to an isotropic cosmic ray flux or possible nearby sources or local magnetic fields. Because of small anisotropy, large data sets are required to make useful measurements which overcome the statistical uncertainties of counting experiments.

A simple way of recording many cosmic rays is to record coincidences between a number of scintillation detectors. Most of such cosmic rays have energies between 100 and 1000 TeV. We have operated a small air shower array on the roof of physics department at Sharif University of Technology in Tehran (35°43′N, 51°20′E, 1200 m $\equiv$ 890 gcm^{-2}) as a prototype for constructing an EAS array on Alborz mountain range at altitude of over 2500 m near Tehran. At the time of writing, more than 234000 showers have been recorded. In the present paper we discuss the design of this scintillator array and describe its operation. The main purpose of experiment is study of anisotropy at energies in the decade below 1 PeV.

Experimental Astronomy **15:** 13–27, 2003.

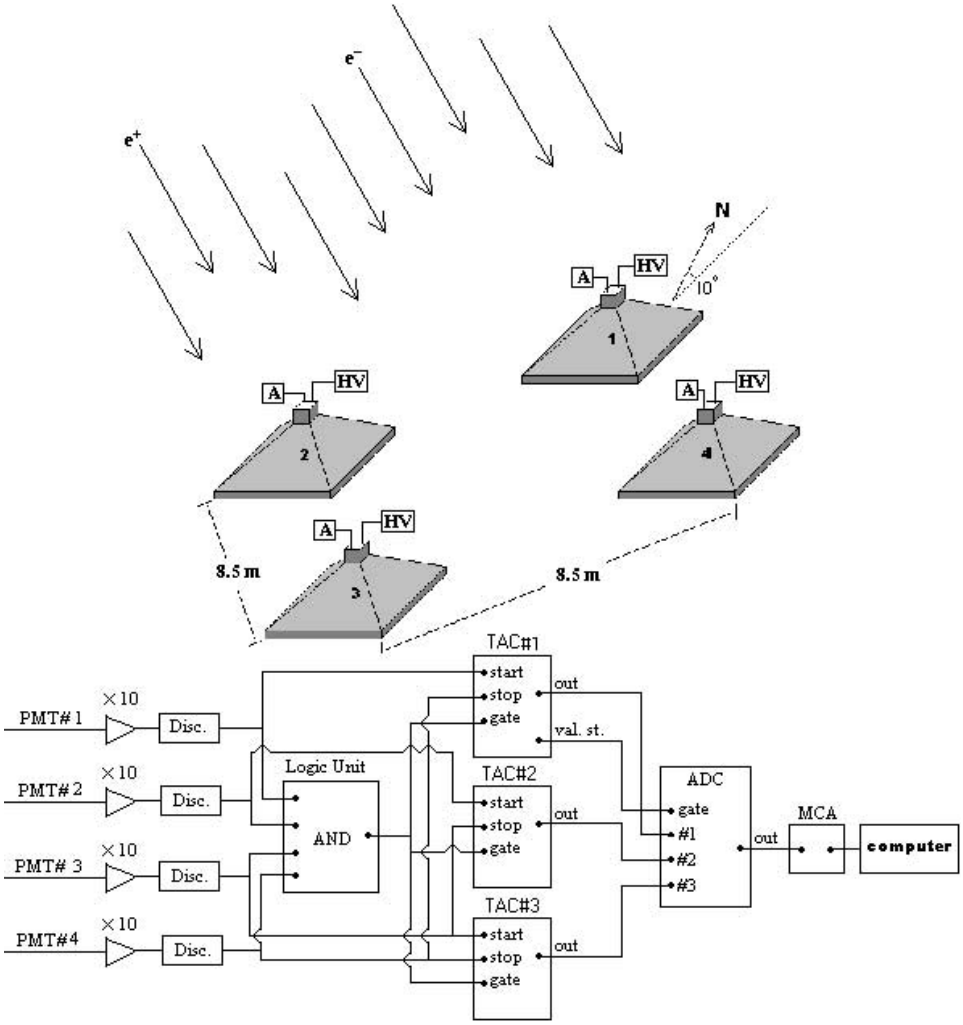

Figure 1. Arrangement of four scintillators as a square array, and its electronic circuit.

2. Description of the array

Four plastic scintillators were used for detection of EASs. Each of the scintillators ($100 \times 100 \times 2\text{cm}^3$) is housed in a pyramidal steal box. Inside of each detector box was painted white (Bahmanabadi et al., 1998). There is a fast photomultiplier (EMI9813KB) of 5 cm diameter above each scintillator. The layout of the array is given in Figure 1. Signals from the PMTs are amplified in one stage ($\times 10$) with a fast amplifier (CAEN N412). Then the signals are connected to an 8- channel fast discriminator (CAEN N413A) which was operated in fixed level of 20 mV. Each channel of the discriminator has two outputs; one of them is connected to a logic unit (CAEN N405) with a gate width of 150 ns, and the other one to a TAC

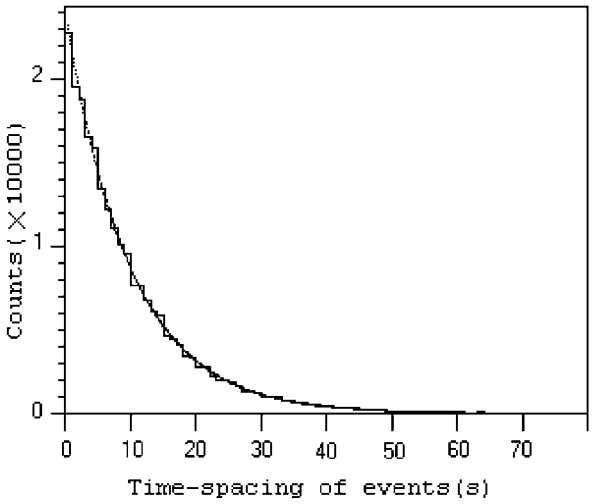

Figure 2. Distribution of events time-spacing.

(ORTEC 566), so that the output of the scintillator No.4 is connected to start input of the TAC No.1, and the output of the scintillator No.2 is connected to the start input of both TAC No.2 and 3. The output of the scintillator No.3 is connected to the stop input of the TAC No.2, and of the scintillator No.1 is connected to the stop input of both TAC No.1 and 3. Then the output of the three TACs which were set to a full scale of 200ns are fed into a Multi Channel Analyzer (MCA) via an Analog to Digital Converter (ADC) unit. When the four scintillators were fired, the apparatus is triggered by logic unit, and time lags between the output signals of the PMTs (4,1), (2,3) and (2,1) are read out by a computer (Figure 1).

3. Array event rate

The data set covers a total period of 2332800 seconds. A total of 234733 events were collected during this time giving a mean event rate of one event every 9.94 seconds. The event time-spacing distribution is shown in Figure 2. Since events occur randomly in time, it is expected that its distribution follows an exponential function,

$$P(t) = A \exp(-t/\tau). \tag{1}$$

The event rate can be obtained by fitting the function on the events time-spacing distribution. One event per every $\tau = 9.84$s is obtained from the fit. Deviation from the exponential law suggested a non-random component for the cosmic ray flux. Bhat et al. (1980) reported a significant deviation from the exponential law, but subsequent investigations failed to confirm this result. For example, the data from the Thebarton array have yielded results consistent with random expectation

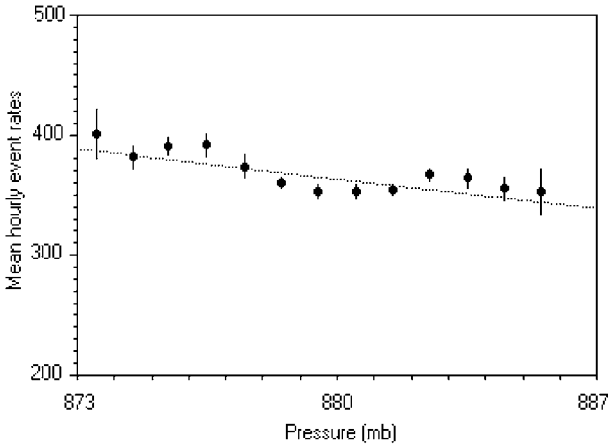

Figure 3. Mean event rates, over all zenith and azimuthal angles and all times, as a function of atmospheric pressure.

(Smith and Clay, 1997). Our observed distribution is also in good agreement with the exponential law.

4. Atmospheric effects on counting rate

The rate of shower detections depends on a number of factors. The Photomultiplier-scintillator combination may have a temperature dependence, but it is not effective on our work, since its variations was very low during the experiment. A more serious problem is the dependence of the detection rate on atmospheric pressure. Pressure data are usually available from the local Meteorological Organization.

In Figure 3 the mean event rates, over all zenith and azimuthal angles and all times, as a function of the atmospheric pressure are shown. Various methods are used in order to study the dependence of event rate on atmospheric pressure (Alexandreas et al., 1993; Horns, 1999). We can describe this mean event rate by the following function

$$R = R_0 \exp\left(\frac{P_0 - P_i}{P_1}\right). \tag{2}$$

The values of $R_0 = 356\text{h}^{-1}$, $P_0 = 882\text{mb}$, and $P_1 = 102\text{mb}$ were obtained from the data (Attention: See the start points of axes in Figure 3). P_i denotes the measured air pressure at a given time. By this empirical function, we weighted the raw event rates for atmospheric pressure.

5. Analysis of anisotropy

For low anisotropies, it is necessary to consider the effect of counting statistics for a finite data set and the effect of count rate variations due to meteorological conditions. The strength and direction of the anisotropy in the arrival directions of the Ultra High Energy cosmic rays can be quantified by harmonic analysis, as originally suggested by Linsley (1975). Consider as data a set of N directions $\theta_1, \theta_2, ..., \theta_N$ such that $0 \leq \theta \leq 2\pi$. For simplicity, only the first (lowest) harmonic is considered. The results apply formally to all harmonics. The first harmonic amplitude, r_{1h}, and phase, θ_{1h}, are defined in Fourier analysis as:

$$r_{1h} = (a_{1h}^2 + b_{1h}^2)^{1/2}, \tag{3}$$

where

$$a_{1h} = \frac{2}{N}\sum_{i=1}^{N}\cos\theta_i \quad , \quad b_{1h} = \frac{2}{N}\sum_{i=1}^{N}\sin\theta_i, \tag{4}$$

and

$$\theta_{1h} = \begin{cases} \theta & \text{if } b_{1h} > 0\,,\, a_{1h} > 0 \\ \theta + \pi & \text{if } a_{1h} < 0 \\ \theta + 2\pi & \text{if } b_{1h} < 0\,,\, a_{1h} > 0, \end{cases}$$

where $\theta = \tan^{-1}(\frac{b_{1h}}{a_{1h}}) \quad , \quad -\frac{\pi}{2} \leq \theta \leq \frac{\pi}{2}.$

The well-known Rayleigh formula for probability of obtaining fractional amplitude greater than r is given by

$$P(>r) = e^{-k_0} \quad , \quad k_0 = r^2 N/4. \tag{5}$$

Where N is the number of events used in the data set. So, a convenient parameter for characterizing the anisotropy amplitude probability distribution is k_0. We can take $\sqrt{2}r_{rms}$ which corresponds to $k_0 = 1$, as noise amplitude.

5.1. Anisotropy in solar and sidereal time

Figures 4 and 5 show the raw number of events detected and weighted for atmospheric pressure as a function of solar and sidereal times, respectively. Table I shows the results of Fourier analysis on the data, both with and without pressure corrections. All harmonics, except the first one in solar and sidereal times of the raw events, are consistent with noise, i.e. the atmospheric pressure variation is clearly visible in both solar and sidereal times. As we have found in the data sets, the pressure corrections make much difference in the final results.

TABLE I
Anisotropy results for raw events and pressure weighted

		First Harmonic			Second Harmonic		
Raw events:	*#events*	$r_{1h}(\%)$	$\theta_{1h}(h)$	k_0	$r_{2h}(\%)$	$\theta_{2h}(h)$	k_0
Solar	234733	1.13	0.61	7.45	0.20	17.71	0.24
Sidereal	234733	1.08	14.13	6.89	0.29	18.17	0.49
Pressure weighted:							
Solar	234733	0.59	0.88	2.05	0.39	18.4	0.88
Sidereal	234733	0.53	6.23	1.65	0.39	5.19	0.88

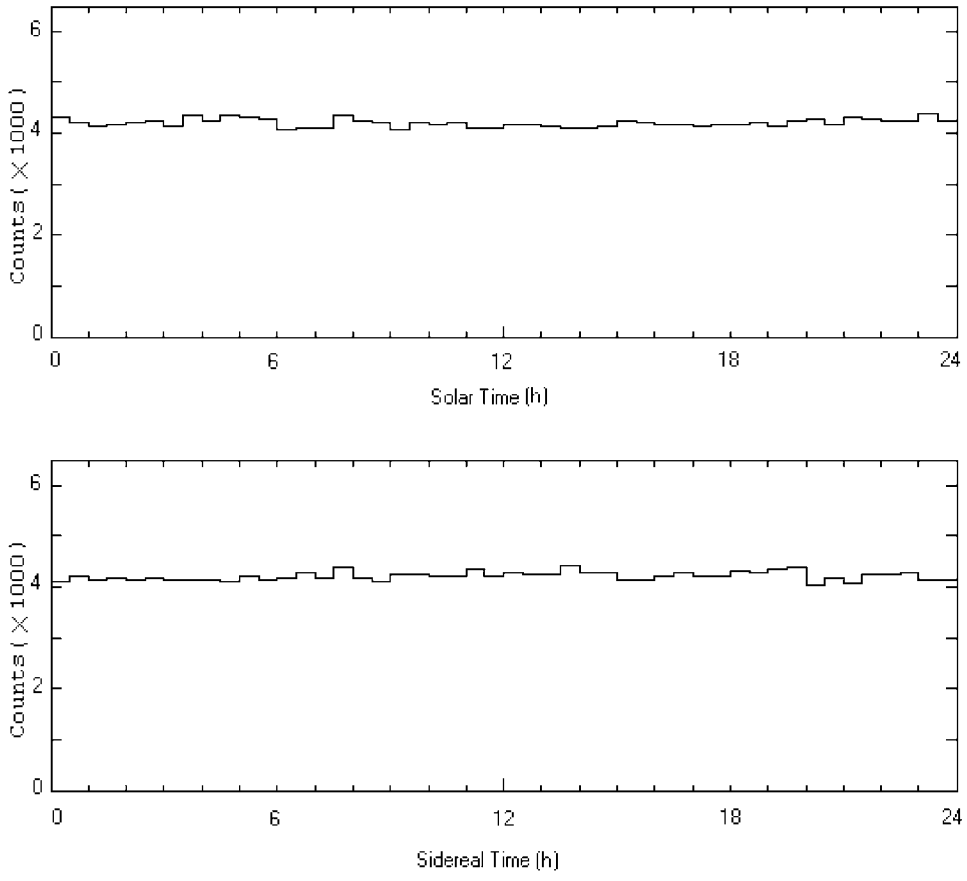

Figure 4. Raw number of events as a function of (a) solar, and (b) sidereal times.

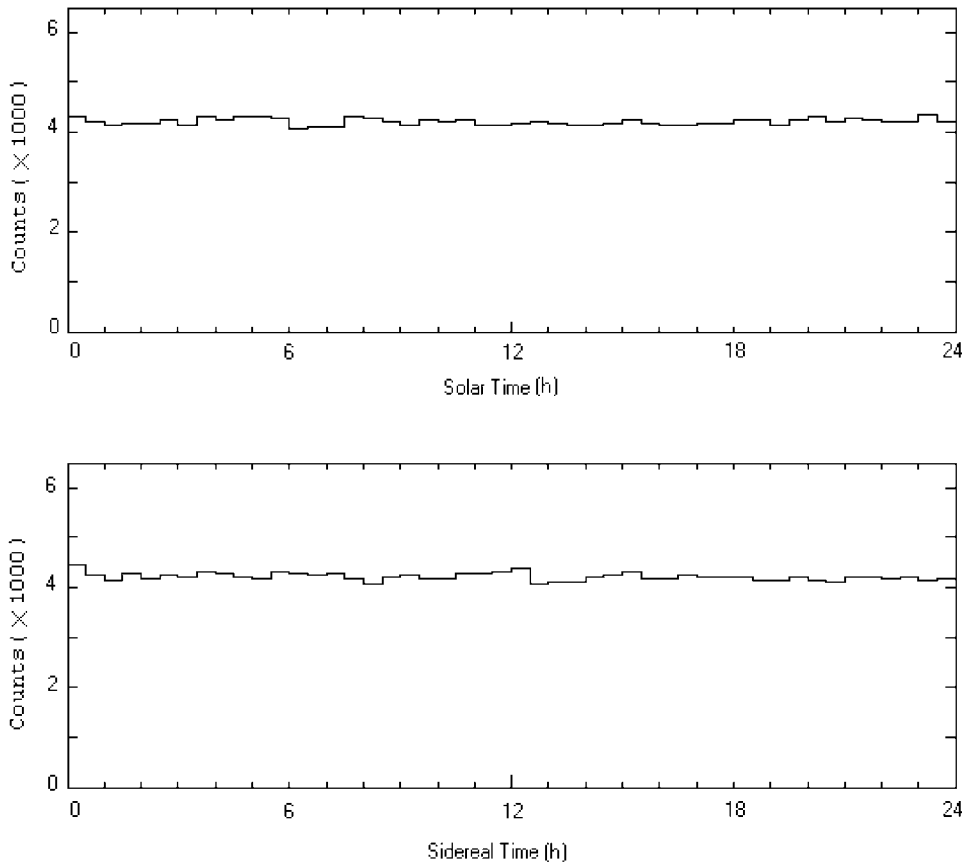

Figure 5. Same as Figure 4 when are weighted to atmospheric pressure.

TABLE II
Anisotropy results for the azimuth angle

	First Harmonic			*Second Harmonic*		
	$r_{1h}(\%)$	$\theta_{1h}(^\circ)$	k_0	$r_{2h}(\%)$	$\theta_{2h}(^\circ)$	k_0
$5^\circ \leq \theta < 20^\circ$	5	182	10	2	212	1.4
$20^\circ \leq \theta < 35^\circ$	11	174	53	1.9	106	1.5
$35^\circ \leq \theta < 50^\circ$	14	183	42	4.6	343	4
all θ	9.4	177	96	1.2	320	1.4

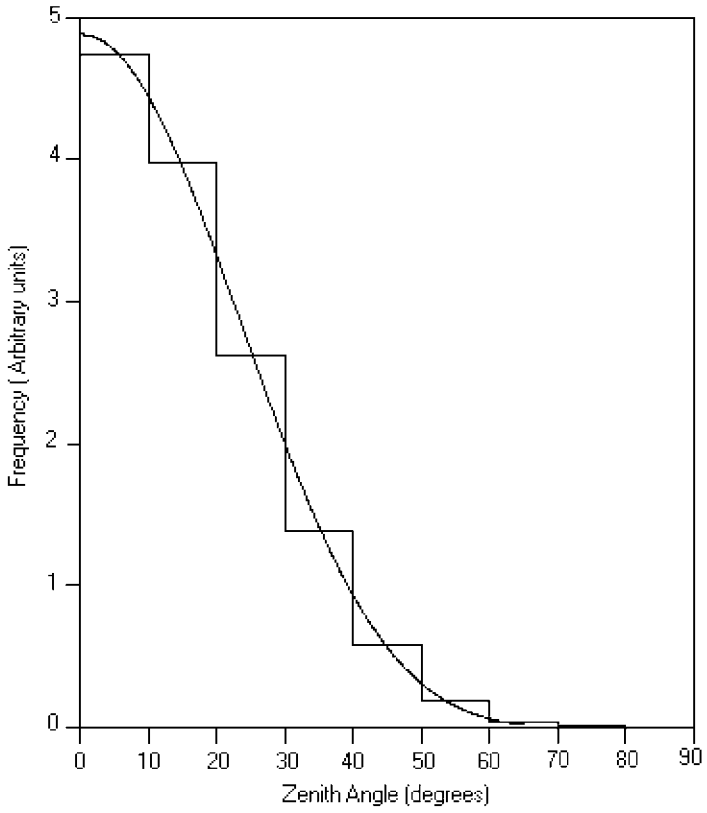

Figure 6. Frequency of showers per solid angle vs. zenith angle, θ.

5.2. ANISOTROPY IN AZIMUTH ANGLE

With arrangement of four scintillators as a square array, Figure 1, we measured the time lag between the detectors (4,1), (2,3) and (2,1) for each shower. Arrival direction of an air shower can be determined by least-square method (Mitsui et al., 1990). It is assumed that the shower axis is perpendicular to the shower front. A set of about 234000 showers was used for this analysis. Figure 6 shows the distribution of zenith angle. The differential zenith angle distribution can be represented by $Z(\theta)d\theta = Constant.\cos^n\theta\sin\theta d\theta$ with $n = 6.2 \pm 0.2$ obtained from the data. The exponent n increases as the shower size, N, or altitude decreases, so that its value at sea level for the range of relativity small shower ($6 \times 10^4 \leq N \leq 5 \times 10^5$) is $n =$ 10.0 (Luorui and Winn, 1984). Figure 7 shows the azimuthal distribution of EAS events with zenith angle in bins $5^\circ - 20^\circ$, $20^\circ - 35^\circ$, $35^\circ - 50^\circ$, and all zenith angles. The total number of EAS events in the zenith angle intervals used in the analysis has been given at the left side in Figure 7. The azimuth distribution shows a north-south asymmetry. This asymmetry was also observed for events above 5×10^{16} eV with the Yakutsk array (Ivanov et al., 1999). Table II shows anisotropy results for

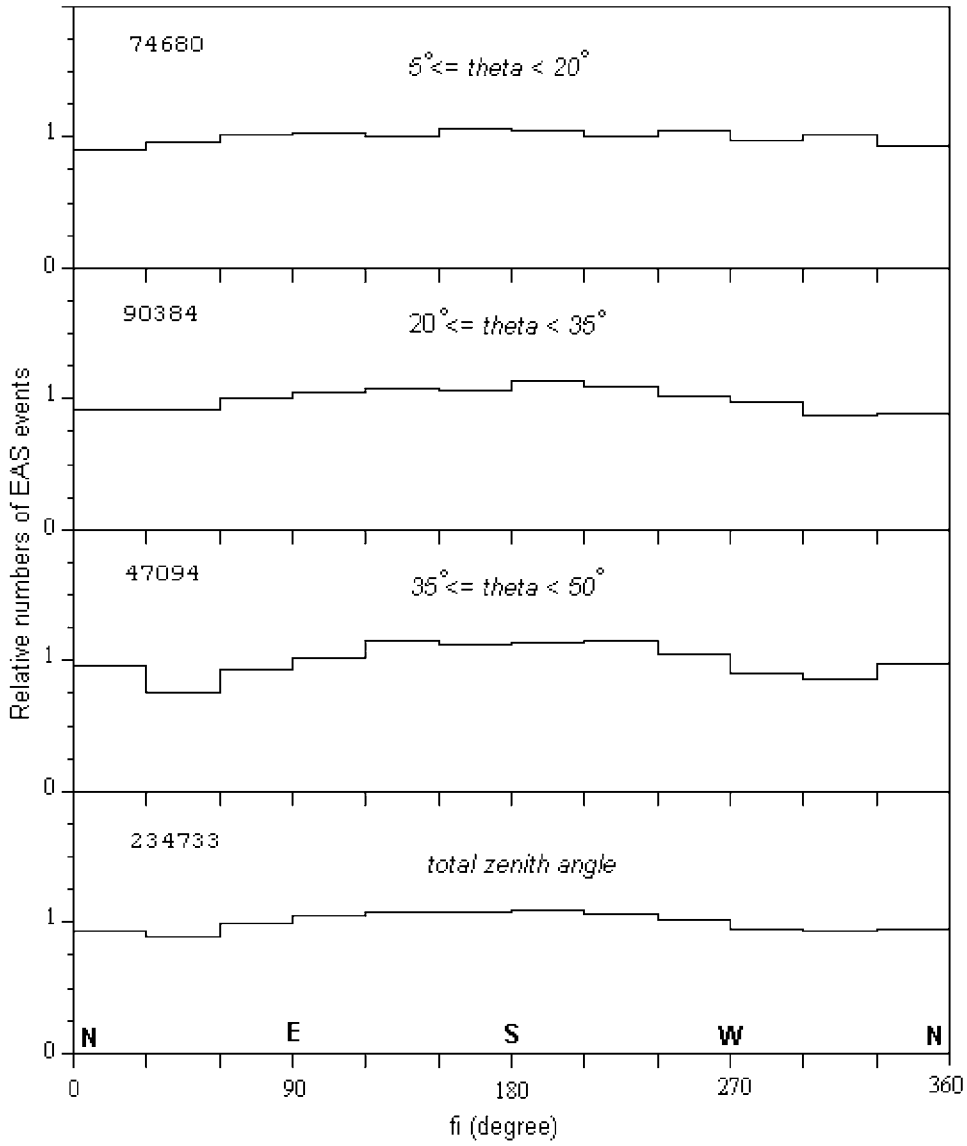

Figure 7. Relative number of events in various zenith angle intervals (shown at each panel).The total number of EAS events in various zenith angles have been given at the left side.

the array. The values of amplitude for the first harmonic are almost always greater than the second harmonic, that is the first harmonics are more important in the array region with the geomagnetic field zenith angle $\theta_H = 38°$. For other arrays the situation may be different. For example, at the Tibet array (30.11°N,90.53°E) where the field zenith angle is $\theta_H = 45°$, both the first and the second harmonics are equally prevailing. At the Yakutsk array (62°N, 130°E; $\theta_H = 14°$) the first

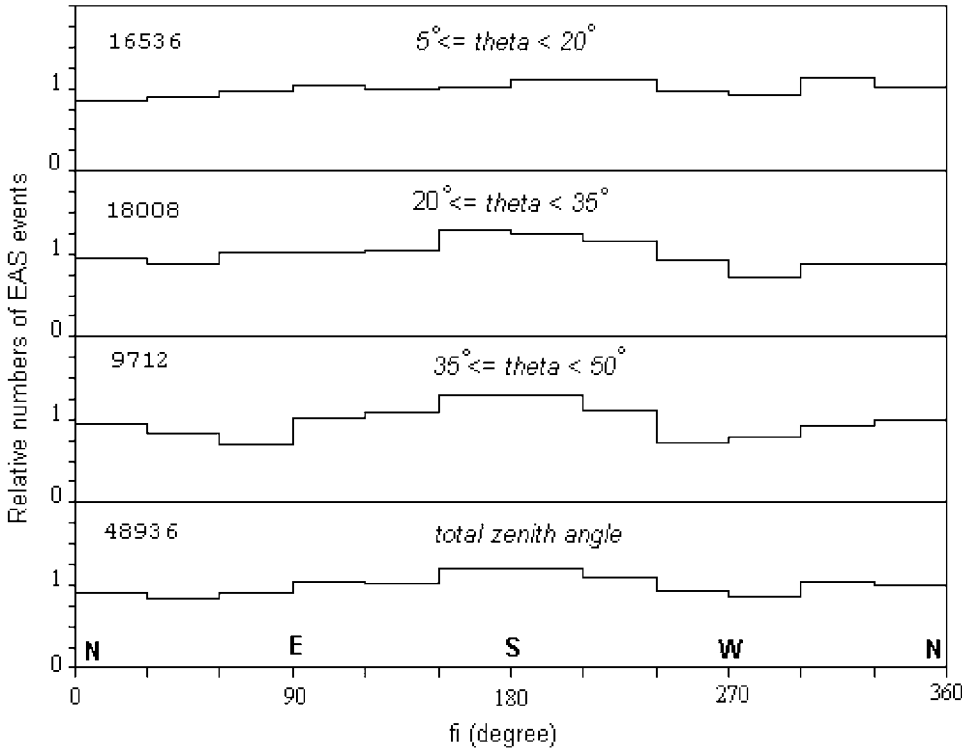

Figure 8. Same as Figure 7 for the experiment with square array rotated 45 degrees.

TABLE III
Results from simulated showers

		First Harmonic			*Second Harmonic*		
	# Counts	$r_{1h}(\%)$	$\theta_{1h}(^\circ)$	k_0	$r_{2h}(\%)$	$\theta_{2h}(^\circ)$	k_0
$\theta < 20^\circ$	4096	3	170	0.92	9.4	125	9.1
$\theta > 20^\circ$	6144	20	171	63	85	306	1107
all θ	10240	9	171	22.7	28	305	197

harmonic, and at the Chakaltaya array (16.35°S, 68.2°W; $\theta_H = 88^\circ$) the second harmonic dominate (Ivanov et al., 1999). In order to demonstrate that this north-south asymmetry is not due to the geometry of our square array we have repeated the experiment with the array rotated by 45 degrees. The azimuth distributions for this experiment exhibit a similar asymmetry as well (Figure 8). This shows that the effect stays fixed in space which is a good evidence for a geomagnetic origin.

We have also used showers simulated by CORSIKA code (Heck et al., 1998) to obtain a rather similar azimuthal distribution. The values of geomagnetic field

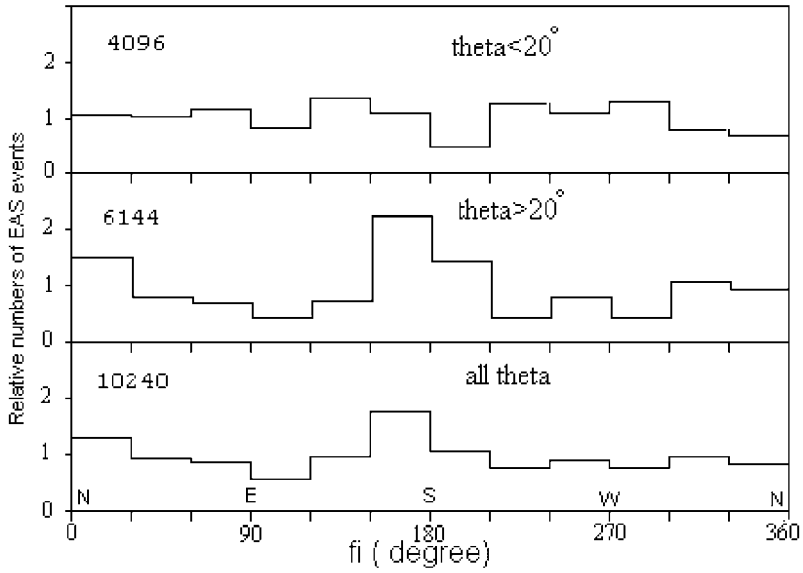

Figure 9. Azimuthal distribution of simulated showers generated by CORSICA code with the values of geomagnetic field of Tehran. The number of simulated showers has been given at the left side.

TABLE IV

Comparison of overall south-north asymmetry of our two experiments and that of simulated showers generated by CORSIKA code $[(N_s - N_n)/(N_s + N_n)(\text{in}\%)]$

Array	$5^\circ \leq \theta < 20^\circ$	$20^\circ \leq \theta < 35^\circ$	$35^\circ \leq \theta < 50^\circ$	$0^\circ \leq \theta < 90^\circ$
Original	3.4	7.2	10	6.4
45° *rotated*	3	11	12	8
Both	3.3	7.8	10.3	6.7
Simulated	2	5	5	3.5

components for Tehran ($B_x = 28.06\ \mu$T, $B_z = 38.37\ \mu$T) were obtained from US Geomagnetic Data Center (see internet address in Refs. 2002). The results for simulated showers is shown in Figure 9. The simulation results for the first and the second harmonics have been given in Table III. The results are clearly consistent with experimental data.

Using the amplitude of $(N_s - N_n)/(N_s + N_n)$, where $N_s(N_n)$ is the number of showers from south (north) half-space, as a function of zenith angle, we have compared the results of our two experiments (Original and 45° rotated) and that of the simulated showers in Table IV for different zenith angle ranges. It is observed that the asymmetry increases with increasing zenith angle, which is consistent with our previous results (Bahmanabadi et al., 2002). This is shown in Figure 10 where

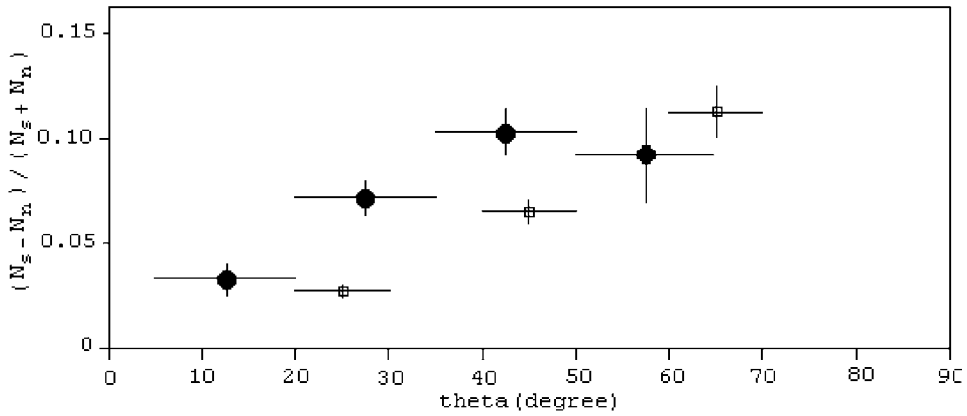

Figure 10. Relative difference of number of showers from south and north half space as a function of zenith angle. Our results (solid circles) have been compared with data of Yakutsk array (squares).

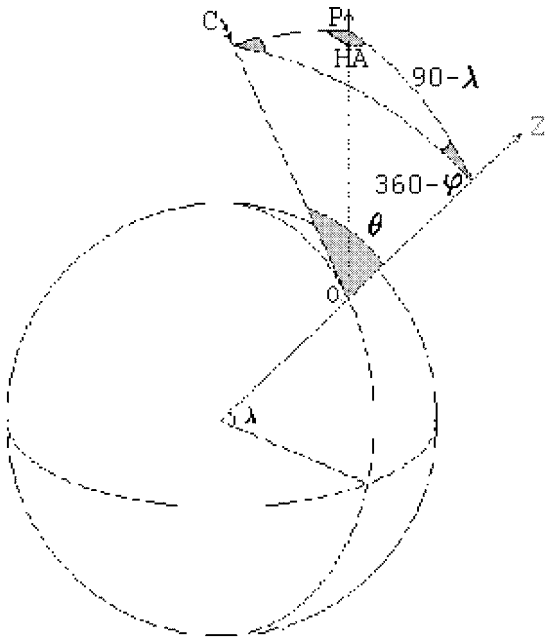

Figure 11. Local and celestial coordinates (see the text).

we have compared our results (solid circles) with data of Yakutsk array (squares). As it is seen from this figure, the asymmetry amplitude increases with θ. In our case this amplitude is more than Yakutsk results, because the geomagnetic field zenith angle in our site is greater than the one in Yakutsk.

5.3. Anisotropy in declination and right ascension angles

The transformation from local to celestial coordinates is calculated as below for an array in the northern hemisphere. The procedure is easily adjusted for arrays south of the equator. In Figure 11, P, C, and Z are the direction of the north pole, the cosmic ray shower axis, and the zenith, respectively. The transformation of coordinates is performed as follows:

1. Using the cosine rule of spherical trigonometry and knowing the colatitude of the array ZP, the zenith angle of the axis ZC (θ), and azimuth angle(φ); compute the codeclination PC.

$$\cos(PC) = \cos(90 - \lambda)\cos\theta + \sin(90 - \lambda)\sin\theta\cos\varphi. \tag{6}$$

2. Using the sine rule and knowing the azimuth, codeclination, and zenith angles of the axis, compute its hour angle (HA),

$$\frac{\sin(HA)}{\sin\theta} = \frac{\sin(360 - \varphi)}{\sin(PC)}. \tag{7}$$

3. Compute the Local Sidereal Time(LST) from $LST = LST_0 + \alpha(ZT - ZT_0)$. LST_0 can be looked up in an almanack for the time ZT_0 (see internet address in Refs. 2002), ZT is the solar time, and α = 1.00273790935 (see internet address in Refs. 2002).
4. Find the Right Ascension (RA) of the axis from $RA = LST - HA$.
5. Declination = 90 - codeclination ($\delta = 90^\circ - PC$).

Accordingly the data was first examined for evidence of any declination anisotropy by comparing the observed declination distribution (Figure 12) with that calculated from the zenith distribution. It was found using a chi-squared test that the probability that the observed data has deviated from isotropy is less than 30%.

The analysis for right ascension was done in three declination bands(δ):

1. $\delta = \lambda$ to $\delta = \lambda + 30^\circ$,
2. $\delta = \lambda - 30^\circ$ to $\delta = \lambda$,
3. $\delta = \lambda - 30^\circ$ to $\delta = \lambda + 30^\circ$.

In these expressions λ is the latitude of array ($35^0 43' N$). The statistical information due to right ascension (Figure 13) has been shown in Table V. The values k_0 in Table V and considering geomagnetic field show that the right ascension distribution of cosmic rays is uniform.

6. Conclusions

The arrival direction of air showers are usually estimated by fast timing shower detection with scintillator arrays. The zenith angle of the arrival direction of air showers obeys a $\cos^n\theta$ law with $n = 6.2 \pm 0.2$. On the other hand, when an air shower arrives at an angle to the earth's magnetic field, the charged particles

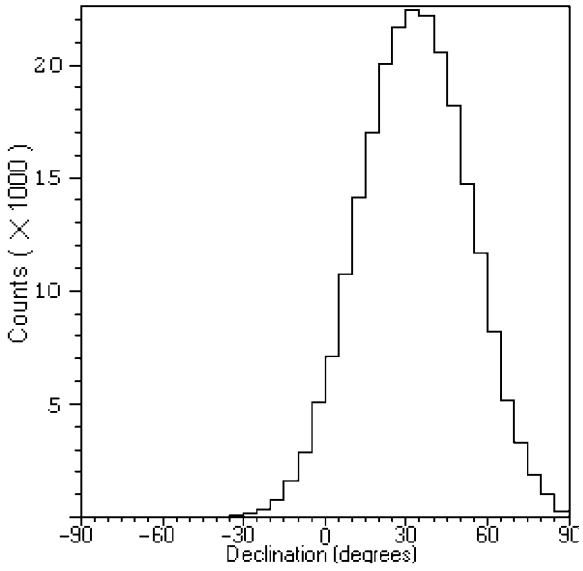

Figure 12. Distribution of EASs vs. declination angle.

TABLE V

Anisotropy results for the right ascension

		$\lambda \leq \delta \leq \lambda + 30^\circ$	$\lambda - 30^\circ \leq \delta \leq \lambda$	$\lambda - 30^\circ \leq \delta \leq \lambda + 30^\circ$
	$r_{1h}(\%)$	0.5	1.1	0.37
First	$\theta_{1h}(^\circ)$	78	273	281
Harmonic	N	94645	109614	204249
	k_0	0.50	3.1	0.7
	$r_{2h}(\%)$	0.24	0.29	0.26
Second	$\theta_{2h}(^\circ)$	314	337	327
Harmonic	N	94645	109614	204249
	k_0	0.14	0.23	0.35

in the cascade can be deflected. Ivanov et al. (1999) have formulated the effect of geomagnetic field on EAS. For showers arriving from the north the shower particles have higher deflections than the southern ones of the equal energy with the equal zenith angle. Thus, it gives the decrease of event rate as it is shown in Figures 7 and 8. The amplitudes of the first two harmonics, can be fitted to $r_I \approx 0.20 \sin^{0.85}\theta \pm 0.03$ and $r_{II} \approx 0.06 \sin\theta \pm 0.01$. Using Fourier analysis of data, and considering pressure corrections, we found no cases that the number of events detected as a function of solar and sidereal times and all subdivisions by declination angle for right ascension differ significantly from random expectation,

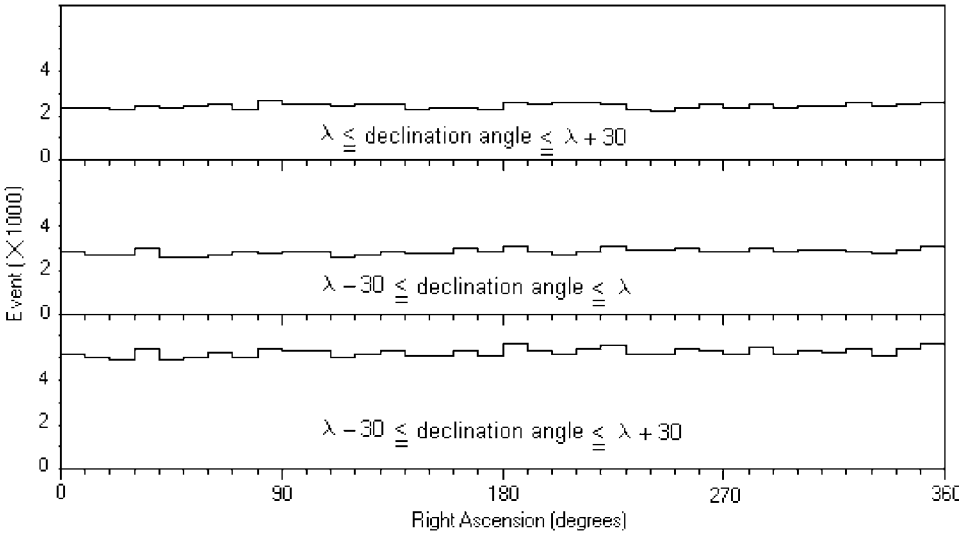

Figure 13. Right ascension distribution in various declination angle intervals (shown at each panel).

at energies in the decade below 1 PeV. The amplitude of the first and the second harmonics right ascension variation is small and consistent with noise.

Acknowledgement

This research has been partly supported by Grant No. NRCI 1853 of National Research Council of Islamic Republic of Iran.

References

Alexandreas, D. E. et al.: 1993, *Nucl. Istr. Meth.* **328**, 570.
Bahmanabadi, M. et al.: 1998, *Experimental Astronomy* **8**(3), 211.
Bahmanabadi, M. et al.: 2002, *Experimental Astronomy* **13**(1),39.
Bhat, C. L., Sapru, M. L. and Kaul, C. L.: 1980, *Nature* **288**, 146.
Heck, D. et al.: 1998, CORSIKA (Cosmic Ray SImulation for KASCADE) FZKA6019 (Forschungszentrum Karlsruhe).
Horns, D.: 1999, 26th ICRC (Salt Lake City), OG 3.2.24 Proc.
http://www.ngdc.noaa.gov/seg/potfld/geomag.html, June 2002
http://tycho.usno.navy.mil/sidereal.html, 2002
Ivanov, A. A et al.: 1999, *JETP Lett.* **69**, 288.
Linsley, J.: 1975, *Phys.Rev. Letts.* **34**, 1530.
Luorui, S. and Winn, M. M.: 1984, *Nucl. Istr. Meth.* **A223**, 173.
Mitsui, K. et al.: 1990, *Nucl. Istr. Meth.* **A290**, 565.
Smith, A. G. K. and Clay, R. W.: 1997, *Aust. J. Phys.* **50**, 827.